CRATER DEGRADATION IN THE MARTIAN HIGHLANDS: MORPHOMETRIC ANALYSIS OF THE SINUS SABAEUS REGION AND SIMULATION MODELING SUGGEST FLUVIAL PROCESSES. N. Forsberg-Taylor[1,2], A. D. Howard[1], R. Craddock[3] [1]Department of Environmental Sciences, University of Virginia, Charlottesville, VA 22903; [2]now at: Earth and Planetary Sciences, Washington University, St. Louis, MO 63130; [3]Center For Earth and Planetary Sciences, Smithsonian Institution, Washington, D.C. 20546

Introduction: The Sinus Sabaeus Quadrangle (0°S to 30°S and 0°E to 45°E) was selected as a representative highly cratered region to characterize the morphometry of 530 fresh and degraded craters greater that 10 km in diameter. Individual MOLA tracks were utilized rather than gridded data to avoid artifacts due to sparse data. An additional 320 craters were included in crater counts but were not morphometrically analyzed because of 1) poor MOLA coverage; 2) strong modification by later impacts, or 3) breaching of the crater wall by entering or exiting fluvial channels (not a closed depositional system). Each crater was visually assigned a degree of degradation using the standard classification system [1,2,3], ranging from 'A' for fresh to 'E' for highly degraded craters. Qualitative characteristics were used in conjunction with the quantitative morphometric measurements to examine the properties of crater modification within the quadrangle as a function of crater diameter, location within the quadrangle and elevation. A variety of measurements and analyses were conducted [4], but we report here results related to determining the processes responsible for degradation.

Relative Crater Depth: One measure of the degree of crater degradation is the relative crater depth, R, which we define as:

$$R = \left(H - h\right) / H \ ,$$

where H is the crater depth (rim to lowest point on the crater floor) for a fresh crater of the observed diameter estimated using statistics from [5], and h is the actual crater depth. The resulting frequency distribution of R for all craters between 10 and 100 km in diameter is strongly bimodal (***Fig. 1***), with craters visually classified as being only slightly degraded (classes A & B) forming the lower peak at R<0.2, whereas more degraded craters (classes C, D, & E) form the peak at 0.4<R<0.9. The size-frequency distribution of craters forming the lower peak (A&B) is consistent with them representing the post-Noachian population of fresh to slightly degraded craters (***Fig. 2***). The size distribution for all craters >30 km in diameter closely follows the highlands curve of [6].

Simulation Modeling: Fresh craters created analytically using geometric statistics [5], and ranging in diameter from 1 to 100 km, were modified by simulated fluvial erosion (***Fig. 3***) [7,8]. The relative time, T, for craters to reach a given degree of degradation measured by R was quantified as a function of crater diameter, D, giving

$$T \propto D^{1.96} R^{2.52} \ . \qquad (1)$$

Slightly different exponents occur for different assumptions about values of process parameters.

Eolian degradation by airfall and sand transport is modeled by heuristic rules that approximate deposition and erosion rates as a function of the degree of "exposure" of a given location, based upon a weighted sum of the gradients between the given point and its surroundings. Locations on ridges or peaks (e.g., crater rims) are slowly eroded whereas sheltered locations are depositional (***Fig. 4)***. The time T to reach a given R for eolian degradation is nearly a linear function:

$$T \propto D^{0.66} R^{0.77} \qquad (2)$$

If crater degradation and crater production were in approximate steady state during the Noachian, then the nearly linear dependency of infilling time with diameter for eolian infilling (2) would imply a nearly uniform frequency distribution of R, whereas for fluvial erosion the rate of infilling decreases sharply with time (1), which would give a negatively skewed frequency distribution of R. The observed frequency distribution of degraded craters in Sinus Sabaeus is negatively skewed (classes C,D, &E in ***Fig. 1***). Therefore the frequency distribution of relative crater depth, R, is more consistent with the primary agent of modification of >10 km craters during the Noachian being fluvial erosion rather than airfall deposition.

The downturn of the frequency distribution of Sinus Sabaeus craters for degradation state beyond R=0.8 (***Fig. 1***) can be attributed to: 1) highly degraded craters are hard to recognize; 2) older craters are more likely to have been modified, breached, or eradicated by later impacts so that crater shape statistics could not be collected.

The steady state model also has implications for the size-frequency distribution of craters. If production and eradication of craters in a given size range are balanced, then the number of observed craters should be proportional to their average survival time, T. If the survival time is a power function of diameter with power μ,

$$T \propto D^{\mu}$$

and the cumulative production rate $\partial N / \partial t$ is a power function of diameter with exponent ϑ, then the observed cumulative number density, N', should be equal to the product of production rate and survival time [9]:

$$N' \propto D^{\vartheta+\mu}$$

Crater counts [7] suggest that ϑ=-1.8 for crater production in the range 1<D< 32 km and ϑ=-2.2 for D>32 km. A synthetic cumulative curve for ancient cratered terrain on Mars [6] (***Fig. 2***) under the assumption that eolian infilling dominates crater degradation in the range of 1 to 50 km gives a slope $N' \propto D^{-1.0}$, roughly consistent with our simulations of eolian sedimentation (2). Fluvial erosion should produce an even stronger reduction in the slope $\vartheta+\mu$ to values approaching zero (using exponents for μ from (1)). The cumulative frequency curve for the Sinus Sabaeus region is strongly convex in the region from 10 km to 70 km with $\partial N/\partial t$ increasing from about -0.16 in the 10-11 km range through -0.76 in the 11-15 km range and about -1.7 in the 30-40 km range to about -3.1 in the 55-65 km range (***Fig. 2***). This suggests a gradual transition from a production or saturation distribution for craters >50 km to a steady state fluvial degradation distribution in the 10-15 km range.

References: [1] Craddock, R. and Maxwell, T. (1993) *JGR, 98,* 3453-68. [2] Craddock, R., Maxwell, T., and and Howard, A (1997), *JGR, 102,* 13321-40. [3] Barlow, N. *et al.* (2000), *JGR, 105,*26733-8. [4] Forsberg, N. (2003) MS Thesis, U. Virginia. [5] Garvin, J. *et al.* (2003) *Mars 6,* Abstract #3277. [6] Hartmann, W. and G. Neukum (2001) *Space Sci. Rev. 96,* 165-94. [7] Howard, A. (1994) *Water Resour. Res., 30,* 2261-85. [8] Craddock, R. and A. Howard (2002) *JGR 107,* doi:10.1029/2001JE001505. [9] Hartmann, W. (1971) *Icarus, 15,* 410.

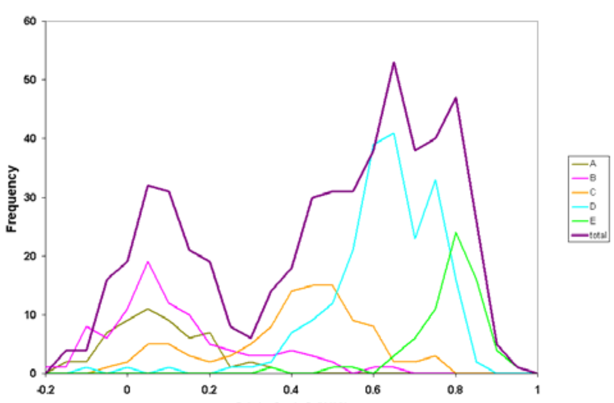

Figure 1. Frequency distribution of relative depth, *R*, for fresh and degraded impact craters in the Sinus Sabaeus Quadrangle. Separate curves are shown for craters falling in the classes A (fresh) to E (highly degraded) as well as the total crater population.

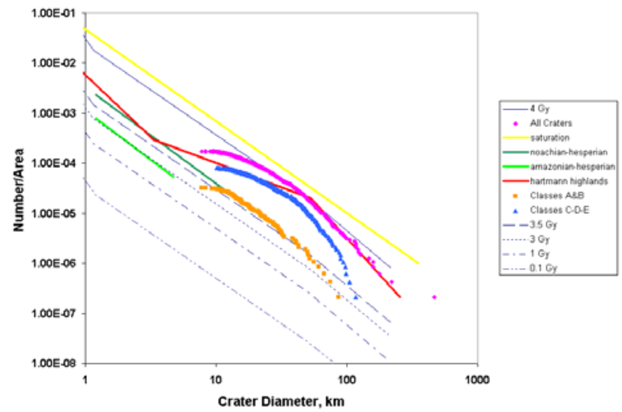

Figure 2. Cumulative size-frequency diagram for impact craters in the Sinus Sabaeus Quadrangle. Purple: all craters greater than about 10 km in diameter; Blue: Ckasses C,D,&E; Gold: A&B; Dark Green: Noachian Hesperian boundary; Light Green: Hesperian-Amazonian boundary: Yellow: Crater saturation; Red: Synthetic highlands curve [6], and inferred age contours from [6].

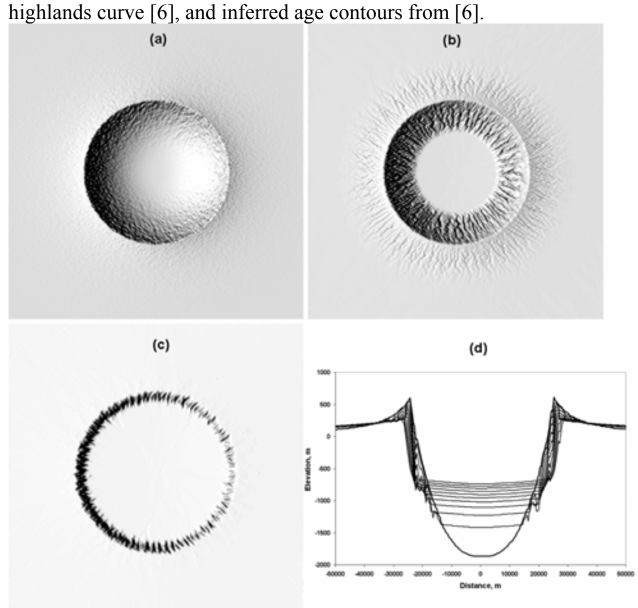

Figure 3. Simulated degradation of a 50 Km impact crater (a) by fluvial erosion, mass wasting, and fluvial sediment deposition. Successive erosion stages shown in (b) and (c). (d) Profiles through the center of the crater at equal temporal intervals.

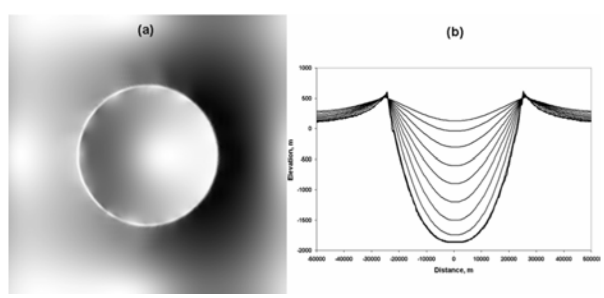

Figure 4. Simulated degradation of a 50 Km impact crater through eolian infilling and erosion. Advanced infilling shown in (a). Profiles through the center of the crater at equal time intervals shown in (b).